An L40C Mutation Converts the Cysteine-Sulfenic Acid Redox Center in Enterococcal NADH Peroxidase to a Disulfide†

Holly Miller,‡ Sharmila S. Mande,§ Derek Parsonage,‡ Steve H. Sarfaty,§ Wim G. J. Hol,§ and Al Claiborne*,‡

Department of Biochemistry, Wake Forest University Medical Center, Winston-Salem, North Carolina 27157, and Department of Biological Structure, Biomolecular Structure Program, and Howard Hughes Medical Institute SL-15, School of Medicine, University of Washington, Seattle, Washington 98195

Received December 14, 1994; Revised Manuscript Received February 8, 1995⊗

ABSTRACT: Multiple sequence alignments including the enterococcal NADH peroxidase and NADH oxidase indicate that residues Ser38 and Cys42 align with the two cysteines of the redox-active disulfides found in glutathione reductase (GR), lipoamide dehydrogenase, mercuric reductase, and trypanothione reductase. In order to evaluate those structural determinants involved in the selection of the cysteine-sulfenic acid (Cys-SOH) redox centers found in the two peroxide reductases and the redox-active disulfides present in the GR class of disulfide reductases, NADH peroxidase residues Ser38, Phe39, Leu40, and Ser41 have been individually replaced with Cys. Both the F39C and L40C mutant peroxidases yield active-site disulfides involving the new Cys and the native Cys42; formation of the Cys39−Cys42 disulfide, however, precludes binding of the FAD coenzyme. In contrast, the L40C mutant contains tightly-bound FAD and has been analyzed by both kinetic and spectroscopic approaches. In addition, the L40C and S41C mutant structures have been determined at 2.1 and 2.0 Å resolution, respectively, by X-ray crystallography. Formation of the Cys40−Cys42 disulfide bond requires a movement of Cys42-SG to a new position 5.9 Å from the flavin-C(4a) position; this is consistent with the inability of the new disulfide to function as a redox center in concert with the flavin. Stereochemical constraints prohibit formation of the Cys41−Cys42 disulfide in the latter mutant.

Enterococcal NADH peroxidase ($NADH + H^+ + H_2O_2 \rightarrow NAD^+ + 2H_2O$) and NADH oxidase ($2NADH + 2H^+ + O_2 \rightarrow 2NAD^+ + 2H_2O$) represent a new class of flavoprotein peroxide reductases within the disulfide reductase family (Claiborne et al., 1992, 1993, 1994). Utilization of the cysteine-sulfenic acid (Cys-SOH)[1] redox center, in contrast to the redox-active disulfides found in the two classes of disulfide reductases (Williams, 1992), represents perhaps the major distinguishing feature in the description of these enzymes. Sequence analyses (Ross & Claiborne, 1991, 1992) have shown that both NADH peroxidase and NADH oxidase exhibit only weak homology (21% identity) to human glutathione reductase (GR); nonetheless, the refined 2.16 Å X-ray structure of the peroxidase (Stehle et al., 1991) shows a chain fold and domain organization very similar to that of GR. Despite the differences in non-flavin redox centers, superposition of the respective FAD-binding domains reveals not only very similar FAD conformations but also nearly identical locations for Cys42 of the peroxidase and Cys63 (the charge-transfer cysteine) of GR. Since sulfenic acids are generally unstable, the active-site environment of NADH peroxidase also serves to stabilize the Cys42-SOH redox center (Claiborne et al., 1993). Three major factors which are thought to contribute to this stabilization of the sulfenic acid (and to the further distinction relative to the GR active site) include the following: (1) the exclusion of other active-site cysteine thiols, (2) intramolecular hydrogen-bonding of Cys42-SOH, possibly involving both His10-NE2 and Cys42-N, and probable ionization of Cys42-SOH to the sulfenate, and (3) an apolar microenvironment and very limited solvent access.

Earlier studies demonstrated (Miller & Claiborne, 1991), through chemical and spectroscopic analyses, that alkylation of the GR interchange thiol (Cys58) leads to an entirely different spectral and kinetic course for the reaction of H_2O_2, compared with that for two-electron reduced GR. Overall, the analysis was consistent with the formation of a stabilized Cys-SOH derivative of the remaining charge-transfer thiol (Cys63) on peroxide oxidation of the reduced, monoalkylated protein (EHR). The rates of H_2O_2 reduction measured with both two-electron reduced (EH_2) and EHR forms of GR, however, fail to support significant catalytic peroxidatic activity. Recent mutagenesis studies with the recombinant NADH peroxidase (Parsonage & Claiborne, 1995) fully support the catalytic redox role of Cys42-SOH, and the X-ray structures of the C42S and C42A mutants at 2.0 Å resolution, avoiding the oxidation of Cys42-SOH to the non-native

† This work was supported by National Institutes of Health Grant GM-35394 (A.C.) and by startup funds from the School of Medicine, University of Washington (W.G.J.H). An equipment grant from the Murdock Charitable Trust is also gratefully acknowledged (W.G.J.H). H.M. was the recipient of a National Science Foundation predoctoral fellowship.

* To whom correspondence should be addressed at Department of Biochemistry, Wake Forest University Medical Center, Medical Center Blvd., Winston-Salem, NC 27157-1016. Telephone: (910) 716-3914.

‡ Wake Forest University Medical Center.

§ University of Washington.

⊗ Abstract published in *Advance ACS Abstracts,* April 1, 1995.

[1] Abbreviations: Cys-SOH, cysteine-sulfenic acid; GR, glutathione reductase; EHR, reduced monoalkylated enzyme; EH_2, two-electron reduced enzyme; IPTG, isopropyl β-D-thiogalactopyranoside; SDS−PAGE, sodium dodecyl sulfate−polyacrylamide gel electrophoresis; DTT, dithiothreitol; DTNB, 5,5′-dithiobis(2-nitrobenzoate); TNB, 5-thio-2-nitrobenzoate; NTSB, 2-nitro-5-thiosulfobenzoate; EH_4, four-electron reduced enzyme; $E'°$, midpoint oxidation−reduction potential at pH 7.

0006-2960/95/0434-5180$09.00/0

Cys42-sulfonic acid (Cys42-SO_3H) observed in the wild-type enzyme structure, have provided additional insights (Mande et al., 1995) regarding both the active-site structure and mechanism of the native enzyme. In this report we have systematically replaced Ser38, Phe39, Leu40, and Ser41 of the NADH peroxidase with Cys, in order to compare the structural and functional properties of resulting active-site disulfide(s) with those of both the native Cys42-SOH redox center and the redox-active disulfides of the GR-like disulfide reductases.

EXPERIMENTAL PROCEDURES

Materials and General Methods. The bacterial strains and other materials used in this work have been described previously (Parsonage & Claiborne, 1995; Parsonage et al., 1993). Anaerobic titrations, enzyme-monitored steady-state kinetics, and thiol and disulfide analyses followed established protocols (Parsonage & Claiborne, 1995; Poole & Claiborne, 1986, 1988). Yeast glutathione reductase was purchased from Sigma and purified by gel filtration chromatography (Miller & Claiborne, 1991). General protocols for DNA isolation and manipulation, mutagenesis, and expression have also been described (Ross & Claiborne, 1991; 1992; Parsonage & Claiborne, 1995).

Sequence Analyses. In order to generate plots of the similarity scores for the GR-like disulfide reductases, a multiple sequence alignment was first performed with 19 representative sequences (glutathione reductases, lipoamide dehydrogenases, mercuric reductases, and one trypanothione reductase) using the GCG program PILEUP (Devereux et al., 1984). This alignment was then imported into the PLOTSIMILARITY program of the GCG suite, which calculates the average similarity among all members of the group of sequences at each position. These results are then plotted as similarity scores *versus* position in the alignment. For the multiple sequence alignment shown (see Results), the program CLUSTAL (Higgins & Sharp, 1988) was used.

Mutagenesis and Expression. The F39C and L40C mutations were generated in the plasmid pNPR4, as recently described (Parsonage & Claiborne, 1995) for Ser and Ala mutants of Cys42. The mutated p39a and p40a plasmids, however, were digested with *Sal*I and *Sph*I, and the resulting 400 bp fragments were transferred directly to the pNPX8 (Parsonage et al., 1993) expression plasmid. The final pF39C and pL40C plasmids, which differ from pC42S and pC42A by the inclusion of approximately 230 bp of native enterococcal sequence upstream of the structural gene, were then sequenced from the *Sph*I site back to the start of the coding sequence. To generate the S38C and S41C mutations, on the other hand, the expression plasmid pNPX9 (Parsonage et al., 1993) was first digested with *Sal*I and *Xba*I to release a 590 bp fragment containing the first 40% of the wild-type *npr* coding sequence. This fragment was ligated directly into pBluescript to generate pNPX14. The S38C and S41C mutations were then generated in this plasmid, the mutant plasmids were digested with *Sal*I and *Sph*I, and the 160 bp fragments were ligated into pNPX9 to give the pS38C and pS41C expression plasmids lacking the 230 bp of upstream enterococcal sequence found in pF39C and pL40C. These plasmids were also checked by both sequence and restriction analysis.

All four mutants were expressed in *Escherichia coli* JM109DE3 on induction with IPTG, and cells were harvested 4 h later. Lower yields were observed with the F39C mutant under these conditions, so cells were harvested at 3 h after induction. The S38C, L40C, and S41C peroxidase mutants were purified following essentially the same protocol described for wild-type and Cys42 mutant enzymes (Parsonage et al., 1993; Parsonage & Claiborne, 1995), but purification of the F39C protein required significant modifications. The gradient volume for the phenyl Sepharose step was reduced from 150 to 110 mL, and the absence of bound FAD required that column fractions be analyzed directly by SDS−PAGE. A 250-mL gradient from 0.2 to 0.35 M NaCl was used to elute the protein from the Q Sepharose column.

All four proteins were purified to at least 95% homogeneity as determined by SDS−PAGE; yields ranged from 31 mg of the F39C protein from 3.5 L of recombinant *E. coli* to 80 mg of the S41C mutant from 3 L of *E. coli*.

Crystallization, Data Collection, and Refinement. Crystals were obtained by the vapor diffusion technique at room temperature. The protein solutions contained 7 and 10 mg/mL concentrations of the L40C and S41C mutants, respectively, in 25 mM potassium phosphate buffer at pH 7.0 with 0.3 mM EDTA and 2 mM DTT. The reservoir contained 1.9 M ammonium sulfate, 5 μM FAD, and 0.1 M potassium phosphate buffer, pH 7.0. A hanging drop of 10 μL was prepared by mixing 5 μL amounts of protein and reservoir solutions. Both mutants crystallized isomorphously with wild-type NADH peroxidase in the orthorhombic space group *I*222 (Stehle et al., 1991). Data for both mutants were collected at room temperature using an X100 Siemens area detector mounted on a RIGAKU (RU200) rotating anode operated at 40 kV and 70 mA, equipped with a graphite monochromator. The crystal-to-detector distance was kept at 100 mm. An oscillation of 0.15° per frame was used. Crystal parameters and data collection statistics are given in Table 1. Data processing, reduction, merging, and scaling were accomplished using the XENGEN software package (Howard et al., 1987). After the final scaling R_{sym} was 0.057 for 44 912 reflections of the L40C mutant, and 0.054 for 51 780 reflections of the S41C mutant.

Table 1: Summary of Crystal and Refined Model Parameters and Data Collection

	L40C	S41C
space group	I222	I222
cell dimensions (Å)		
a	77.7	77.3
b	134.6	134.8
c	145.6	145.8
resolution (Å)	2.1	2.0
completeness of data (%)		
cumulative	91.7	85.9
last shell	80.0 (2.13−2.00 Å)	69.7 (2.04−2.00 Å)
unique reflections obtained	44 912	51 780
merging *R* factor[a] (%)	5.7	5.4
no. of unique reflections used for refinement[b]	37 571	39 181
resolution range (Å)	8.0−2.1	8.0−2.0
rms deviations in		
bond lengths (Å)	0.011	0.012
bond angles (deg)	2.6	2.7
impropers (deg)	1.1	1.3
dihedrals (deg)	25.7	25.8
R factor[c] (%)	17.0	17.4
no. of water molecules	244	252

[a] Merging *R* factor = $\Sigma |I - \langle I \rangle| / \Sigma \langle I \rangle$. [b] Only reflections with $F > 2\sigma(F)$. [c] *R* factor = $\Sigma ||F_o| - |F_c|| / \Sigma |F_o|$.

The starting model used for the refinement of both mutants was the wild-type structure (Stehle et al., 1991). In order to avoid model bias for the side chains of residues 40 and 41 in the L40C and S41C mutants, respectively, these residues were converted into glycines. The triply oxidized Cys42 of the wild-type structure was also converted into glycine by deleting C^{β}, S^{γ}, and the three oxygens of the oxidized cysteine from the atomic coordinates. The starting *R* factors at this stage were 35.3% and 22.0% for the L40C and S41C mutants, respectively. Crystallographic refinement of positions and individual *B* factors was carried out by using the program XPLOR (Brünger et al., 1987) using the conjugate gradient option. Only reflections with $F > 2\sigma(F)$ and with Bragg spacings between 8.0 and 2.1 Å (L40C) and between 8.0 and 2.0 Å (S41C) were used in the refinement. σ_A weighted maps (Read, 1986) with coefficients $||F_o| - |F_c|| \exp(i\phi_c)$ and $2m|F_o| - D|F_c| \exp(i\phi_c)$, where ϕ_c is the calculated phase from the model, were displayed on a Silicon Graphics workstation using the program O (Jones et al., 1991). The maps for L40C clearly showed densities for cysteines corresponding to residues 40 and 42. In the S41C mutant the map clearly showed the density of the triply oxidized Cys42 and of the mutated residue 41. Before further refinement, residue 42 was then changed to Cys in L40C and to triply oxidized Cys in the S41C mutant. Residues 40 and 41 were changed to Cys in the L40C and S41C mutants, respectively. Water molecules were identified by searching peaks above three standard deviations from the mean in an $||F_o| - |F_c||$ map with the program PEKPIK from the XTAL package (Hall & Stewart, 1987). It was ensured that the distance of each of these peaks from the nearest protein atom was not less than 2.5 Å and not more than 3.5 Å. Before accepting them in the models, they were inspected on the graphics system to check that they formed good hydrogen bonds. Two of the solvent peaks in L40C and one peak in S41C had a tetrahedral appearance. Since the crystals were grown using ammonium sulfate, these peaks were considered likely to be sulfate ions instead of waters. They were not, however, included in the models at this stage of the refinement. The water molecules were assigned arbitrary *B* factors of 30 Å^2. After carrying out several additional cycles of positional and *B*-factor refinement, the $||F_o| - |F_c||$ maps clearly showed three strong peaks in the putative sulfate positions at 4σ above mean electron density. All three peaks, two in L40C and one in S41C, were subsequently treated as sulfate ions. After a total of 280 conjugate gradient cycles, the refinements converged at *R* factors of 17.0% and 17.4%, respectively, for the L40C and S41C mutants. Table 1 gives the refinement results.

The atomic coordinates for the L40C and S41C mutants have been deposited with the Brookhaven Protein Data Bank (identification codes 1NHR and 1NHS, respectively).

RESULTS

Sequence Comparisons. A multiple sequence alignment (not shown) comparing flavoprotein disulfide reductases of the GR class (glutathione reductase, lipoamide dehydrogenase, trypanothione reductase, and mercuric reductase (Williams, 1992)) identified three conserved elements within the respective FAD-binding domains. These correspond to the ADP-binding $\beta\alpha\beta$-fold (Wierenga et al., 1986), the highly conserved sequence corresponding to the redox-active disulfide, and a third segment, consisting of residues Leu136–Pro143 in *E. coli* GR, found at the boundary of the FAD- and NAD(P)-binding domains. The *E. coli* GR structure (Mittl & Schulz, 1994) shows that this latter segment spans the junction between two β-strands (*a4* and *f1*) which connect the two nucleotide-binding domains; *a4* is hydrogen-bonded to two other β-strands within the FAD domain, while the *f1* strand is hydrogen-bonded to the β-strand found at the end of the NADP domain. This conserved element therefore contributes both to β-sheet structures found within the FAD- and NAD(P)-binding domains and to the junction connecting the two domains.

As shown in Figure 1, a similar alignment including the enterococcal NADH peroxidase and NADH oxidase, along with the four disulfide reductases of the GR class, offers an instructive comparison between the two respective flavoprotein classes. While the segments of the NADH peroxidase corresponding to the $\beta\alpha\beta$-fold (A) and interdomain junction (C) agree reasonably well (~70%) with the consensus sequences, the region including the active-site Cys-SOH (B) does not. Residues Ser38–Cys42 of the peroxidase, which correspond to Cys42–Cys47 in the *E. coli* GR sequence, are not associated with any well-defined element of secondary structure (Figure 2). This contrasts with the unusual distorted helix in GR that contributes to the strained conformation of the redox-active disulfide (Karplus & Schulz, 1987). As a result, the distances between Cys42-CA of the peroxidase and the corresponding atoms of Ser38 and Phe39 are 11.1 and 8.8 Å, respectively (Table 2). Since the consensus C^{α}–C^{α} and C^{β}–C^{β} distances required for disulfide formation between two cysteines are ≤6.5 and ≤4.5 Å, respectively (Sowdhamini et al., 1989), these observations suggest that the occurrence of cysteine residues in either of these positions would not yield protein disulfides without significant perturbation of active-site structure.

Mutant Peroxidase S38C. As expected based on these analyses, the NADH peroxidase S38C mutant does not contain a protein disulfide. As observed with recombinant wild-type peroxidase (Parsonage et al., 1993), the S38C mutant as purified consisted largely of the EH_2 (Cys42-SH) redox form which, when titrated with substoichiometric H_2O_2, gave a visible spectrum similar to that of oxidized wild-type enzyme. Anaerobic NADH titration gave rise to both EH_2 and EH_2•NADH species analogous to those seen with wild-type peroxidase (data not shown). The activity of the S38C mutant, as measured in the standard NADH peroxidase assay, was similar (157 units/mg) to that of the wild-type enzyme (115–125 units/mg) as well. NADH peroxidase contains no DTNB-reactive thiols in the oxidized form (Poole & Claiborne, 1986), but thiol assays (Riddles et al., 1979) of the S38C mutant, under nondenaturing conditions, gave an average of 0.63 thiols/FAD in a slow monophasic reaction ($t_{1/2}$ = 4.5 h at 23 °C). The substoichiometric release of TNB was shown to be due to a subsequent competing reaction between nascent TNB and Cys42-SOH, yielding the mixed disulfide. Evidence supporting this interpretation was provided by the observation that, following removal of excess DTNB and TNB over a spin column, the addition of dithiothreitol to the recovered protein yielded 1.1 free TNB/FAD. These results are consistent with the presence of a single free thiol, contributed by Cys38-SH, in the S38C peroxidase.

Another approach for determination of thiol and/or disulfide content in both wild-type and mutant peroxidases

```
                  1       A    |                     |         |   B    |
Nox E.faecalis    MK------VVVVGCTHAGTSAV----------KSILANHPEAEVTVYERNDNISF-LSC-
Npx E.faecalis    MK------VIVLGSSHGGYEAV----------EELLNLHPDAEIQWYEKGDFISF-LSC-
GR  E.coli        MTK--HYDYIAIGGGSGGIASI-NRAAMYGQKCALIEAKE---------LGGTCVNVGCV
Lpd E.coli        -STEIKTQVVVLGAGPAGYSAAFRCADL-GLETVIVER--------YNTLGGVCLNVGCI
MR  S.aureus      FNRDGDYDLLIIGSGGAAFSAAIKANEN-GAKVAMVER---------GTVGGTCVNIGCV
TR  T.congo       MSK--AFDLVIIGAGSGGLEAGWNAATLYKKRVAVVDVQTVHGPPFFAALGGTCVNVGCV
                  .       . .* . .. ..             ...           . ..   ..*

                  43      |            |              |         |
Nox E.faecalis    -GIALYVGGVVKNAADLF---Y-----SNPEELASLGATVKMEHNVEEIN----------
Npx E.faecalis    -GMQLYLEGKVKGVNSVR---Y-----MTGEKMESRGVNVFSNTEITAIQ----------
GR  E.coli        PKKVMWHAAQIREAIHMYGPDYG--FDTTINKFNWETLIASRTAYIDRIHTS-YENVL-G
Lpd E.coli        PSKALLHVAKVIEEAKALAEH---GIVFGEPKTDIDKIRTWKEKVINQLTGG-LAGMAKG
MR  S.aureus      PSKTMLRAGEINGLAQNNPFT---GLQTSTGAADLAQLTEQKDGLVSQMRQEKYIDLIEE
TR  T.congo       PKKLMVTGAQYMDQLRE-SAGFGWEFDASTIKANWKTLIAAKNAAVLDINKS-YEDMFKD
                     .   .   .              .    .         .  .  .

                              84     |        |         C|         |
Nox E.faecalis    -------------VDDKTVTAKNLQTGATET---VSYDKLVMTTGSWPIIPP-IPGIDAE
Npx E.faecalis    -------------PKEHQVTVKDLVSGEERV---ENYDKLIISPGAVPFELD-IPGKDLD
GR  E.coli        KNNVDVIKGFARFVDAKTLEVNG---------ETITADHILIATGGRP-SHPDIPGVEYG
Lpd E.coli        R-KVKVVNGLGKFTGANTLEVEGENG-----KTVINFDNAIIAAGSRPIQLPFIPH-EDP
MR  S.aureus      Y-GFDLIRGEASFIDDKTIQVNGQN---------ITSKSFLIATGASP-AVPEIPGMNEV
TR  T.congo       TEGLEFFLGWGALEQKNVVTVREGADPKSKVKERLQAEHIIIATGSWP-QMLKIPGIEHC
                                 . . . .                .  ....*. *    **  .
```

Figure 1: CLUSTAL alignment (Higgins & Sharp, 1988) corresponding to the FAD-binding domains of *E. faecalis* NADH oxidase (Nox; Ross & Claiborne, 1992) and NADH peroxidase (Npx; Ross & Claiborne, 1991). Also included are sequences for the *E. coli* glutathione reductase (GR; Greer & Perham, 1986) and lipoamide dehydrogenase (Lpd; Stephens et al., 1983), *Staphylococcus aureus* mercuric reductase (MR; Laddaga et al., 1987), and *Trypanosoma congolense* trypanothione reductase (TR; Shames et al., 1988). Boxes A−C correspond to the ADP-binding $\beta\alpha\beta$-fold, the redox-active disulfide, and the interdomain segments, respectively, of the disulfide reductases. The secondary structural elements corresponding to these regions in *E. coli* GR (Mittl & Schulz, 1994) are also designated. Further details are given in Results.

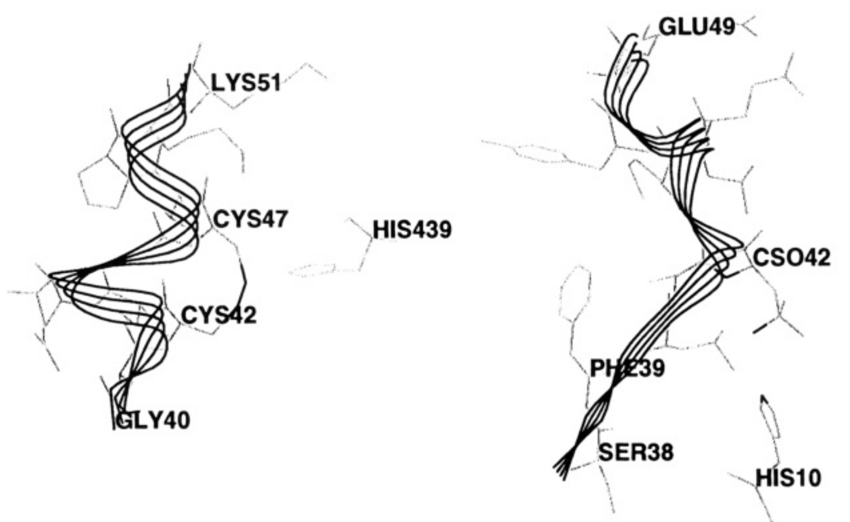

Figure 2: Comparison of the active-site structures of *E. coli* glutathione reductase (left; Mittl & Schulz, 1994) and *E. faecalis* NADH peroxidase (right; Stehle et al., 1991). In *E. coli* GR, Cys42 and Cys47 comprise the redox-active disulfide; Cso42 represents the non-native Cys42-SO_3H derivative of the sulfenic acid in the peroxidase structure. These segments correspond to the box labeled "B" in Figure 1.

involves the reagent NTSB (Thannhauser et al., 1984) which, in the presence of 0.1 M sulfite under denaturing conditions, reacts both with existing thiols and with nascent thiols generated by sulfitolysis of disulfides. The wild-type enzyme gives no reaction with NTSB under these conditions (Poole & Claiborne, 1988). With the S38C mutant, however, a distinctly biphasic increase in absorbance at 412 nm is observed; the slow phase ($t_{1/2}$ = 0.9 min) accounts for release of 0.37 TNB/FAD. The faster phase corresponds to 0.53 TNB/FAD, giving an overall stoichiometry of 0.9 TNB/FAD. In the presence of sulfite, under the denaturing conditions employed, any mixed disulfide (or protein disulfide) resulting from reaction of either Cys42-SOH with TNB or of Cys38-SH with Cys42-SOH will undergo sulfitolysis, ultimately yielding one TNB per disulfide. In order to provide a basis for distinguishing free thiol *versus* disulfide reactivity in the NTSB assay, purified yeast glutathione reductase was analyzed independently. The native enzyme contains five half-cystines per FAD, two of which form the redox-active disulfide (Miller & Claiborne, 1991). The NTSB reaction

Table 2: Active-Site Interatomic Distances in Wild-Type NADH Peroxidase

residues	$C^{\alpha}-C^{\alpha}$ (Å)	$C^{\beta}-C^{\beta}$ (Å)
Ser38−Cys42[a]	11.1	11.5
Phe39−Cys42	8.8	9.7
Leu40−Cys42	5.3	5.1
Ser41−Cys42	3.9	5.7

[a] The multiple sequence alignment given in Figure 1 shows that NADH peroxidase residues Ser38 and Cys42 align with Cys42 and Cys47, the interchange and charge-transfer thiols forming the redox-active disulfide in *E. coli* glutathione reductase. The Cys42−Cys47 $C^{\alpha}-C^{\alpha}$ and $C^{\beta}-C^{\beta}$ distances in *E. coli* GR are 4.6 and 4.1 Å, respectively.

with GR is also biphasic, and the slow phase ($t_{1/2}$ = 3.3 min) accounts for 0.9 of the 4.2 total TNB/FAD released. This result suggests that the fast-reacting component corresponds to the 3 Cys-SH/FAD in GR and is supported by the similar NTSB reaction rates for lysozyme ($t_{1/2}$ = 1.7 min; four disulfides) and the slow phase in the GR reaction taken to represent the single disulfide. Taken together, these results suggest that the biphasic NTSB reaction observed with the NADH peroxidase S38C mutant is composed of a faster, free Cys38-SH reaction and a slower phase attributed to disulfide(s) formed rapidly on denaturation.

The F39C Disulfide Mutant. Expression and purification of the F39C peroxidase mutant immediately revealed the absence of bound FAD. Since the protein has no catalytic activity, SDS−PAGE provided the sole basis for analysis of purity; a modified protocol was adapted in order to optimize the purification. The apoprotein form of the F39C mutant gave no indication of denaturation and/or precipitation over time, however, when stored at 4 °C in a pH 7.0 phosphate buffer with EDTA. An extinction coefficient of 65.8 mM^{-1} cm^{-1} at 280 nm was determined for the pure protein, using the microbiuret protein assay (Bailey, 1962) with bovine serum albumin as the standard. Independent thiol assays of the F39C mutant using DTNB with different preparations, in the presence of 4 M guanidine, gave <0.01, 0.09, and 0.2 TNB/subunit. When assayed for disulfides following the NTSB method described previously, the F39C apoprotein yielded 1.22 and 1.3 TNB/subunit, and essentially all of the absorbance change corresponded to a single monophasic process ($t_{1/2}$ = 4 min). These results indicate that, unlike the S38C mutant, substitution of Cys for Phe39 does lead to the formation of an intramolecular disulfide with Cys42. While the Phe39-CG−Cys42-SG distance in the wild-type peroxidase structure is 9.2 Å, the average S−S bond length in a cystine disulfide is 2.0 Å (Sowdhamini et al., 1989). It seems likely, therefore, that the formation of the Cys39−Cys42 disulfide in the F39C mutant introduces significant structural changes in the active site which preclude FAD binding.

In order to corroborate the presence of the Cys39−Cys42 disulfide and to test whether its formation directly interferes with FAD binding, the effect of DTT on the F39C apoprotein was investigated. A reconstitution protocol, in which the protein was incubated for 10 min at 23 °C with 27 mM DTT and 0.5 mM FAD (~15-fold excess over apoprotein), was developed. Following removal of excess FAD over either a spin column or CM-30 microconcentrator in the presence of 2 mM DTT, the reconstituted holoenzyme form of F39C was obtained, as shown in Figure 3. Although no direct

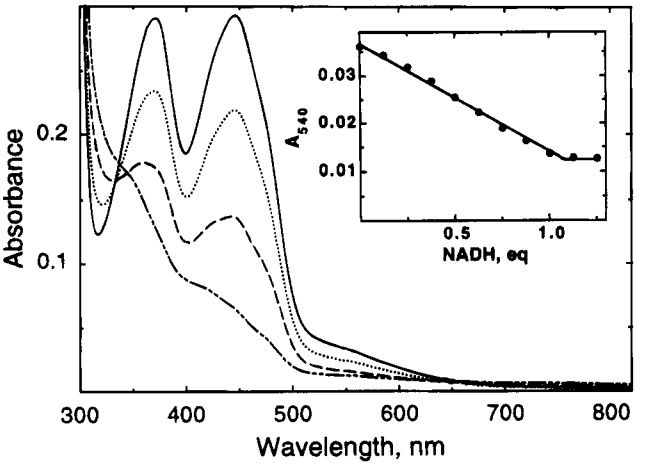

FIGURE 3: Anaerobic NADH titration of the DTT-reconstituted F39C peroxidase. The protein was reconstituted as described in the text; the cuvette contained 18 nmol of enzyme (FAD) in 0.6 mL of 50 mM potassium phosphate, pH 7.0, containing 0.6 mM EDTA and 2 mM DTT. Spectra shown correspond to the addition of 0 (—), 0.5 (•••), 0.88 (- - -), and 1.38 (-•••) equiv of NADH/FAD. Inset: Absorbance change at 540 nm *versus* added NADH.

quantitation of FAD content was attempted, the absorbance ratio of 7.2 at 280 and 450 nm compares favorably with those of both wild-type and S38C mutant enzymes (7.8−8.0 for the respective oxidized enzymes). Furthermore, the visible spectrum of holo-F39C clearly resembles those of the EH_2 forms of wild-type peroxidase (Poole & Claiborne, 1986) and other GR-like disulfide reductases (Williams, 1992), consistent with reduction of the active-site disulfide by DTT. Also, the charge-transfer band centered at 540 nm indicates that, in the EH_2 form, Cys42-SG is both ionized to the thiolate and maintained in the proper juxtaposition relative to the flavin, analogous to the wild-type peroxidase. Taking an extinction coefficient at 450 nm of 9.66 mM^{-1} cm^{-1} as determined for wild-type EH_2 (Poole & Claiborne, 1986), the anaerobic NADH titration shown in Figure 3 requires 1.1 equiv of NADH/FAD and leads to direct flavin reduction in the F39C holoenzyme. This contrasts with the behavior of wild-type EH_2 and suggests that the FAD redox potential (EH_2/EH_4) in holo-F39C is more positive than that of the two-electron reduced wild-type peroxidase.

Since reduction of the Cys39−Cys42 disulfide is required for FAD binding, a protocol for reconstitution employing sulfitolysis in the presence of 1 mM sulfite (replacing DTT) was developed. The visible spectrum of the resulting holo-F39C was more like that of a simple oxidized flavoprotein, however, and lacked charge-transfer absorbance at longer wavelength (data not shown). NADH titration, while reducing the flavin directly, did not yield any EH_2-like intermediate. We conclude that, although sulfitolysis of the Cys39−Cys42 disulfide does allow FAD binding, chemical and/or conformational properties of the resulting holo-F39C protein preclude regeneration of a functional Cys42-SH charge-transfer donor.

The L40C Disulfide Mutant. Sowdhamini et al. (1989) have developed a method for modeling disulfide bonds into proteins of known three-dimensional structure, relying primarily on C^{α} and C^{β} coordinates, and their distance criteria are most nearly satisfied by the Leu40−Cys42 pair in NADH peroxidase (Table 2). As purified, the L40C mutant contains tightly bound FAD, and the absorbance ratio of 7.8 at 280 and 450 nm is very similar to that of both wild-type and

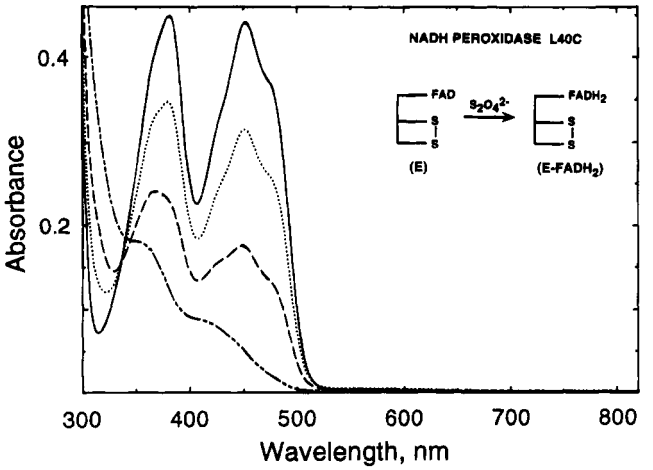

FIGURE 4: Anaerobic dithionite titration of the L40C peroxidase. The cuvette contained 22 nmol of enzyme (FAD) in 0.6 mL of 50 mM potassium phosphate, pH 7.0, plus 0.6 mM EDTA. Spectra shown correspond to the addition of 0 (—), 0.27 (•••), 0.54 (- - -), and 1.08 (-•••-) equiv of dithionite/FAD.

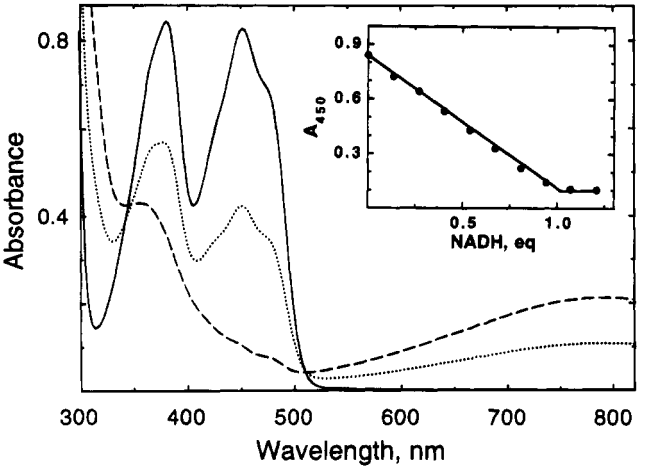

FIGURE 5: Anaerobic NADH titration of the L40C peroxidase. The cuvette contained 43 nmol of enzyme (FAD) in 0.6 mL of the standard pH 7.0 phosphate buffer containing EDTA. Spectra shown correspond to the addition of 0 (—), 0.54 (•••), and 1.07 (- - -) equiv of NADH/FAD. Inset: Absorbance change at 450 nm *versus* added NADH.

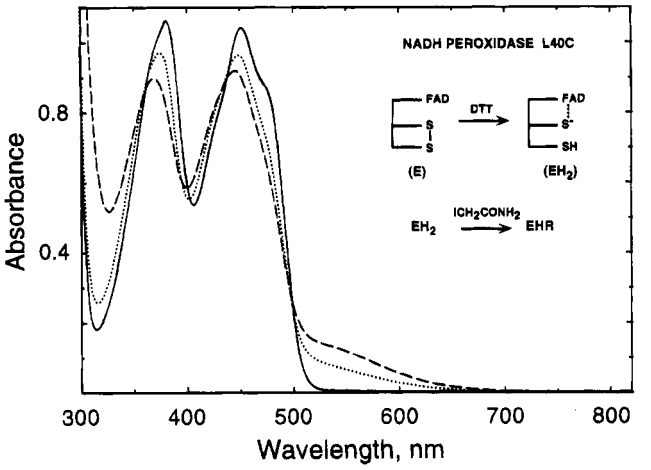

FIGURE 6: Anaerobic DTT reduction and alkylation of the L40C peroxidase. The cuvette contained 58 nmol of enzyme (FAD; —) in 0.7 mL of the standard pH 7.0 phosphate/EDTA buffer. After anaerobiosis, 7 μL of 0.5 M DTT was added from one side arm, and the final DTT-reduced L40C spectrum (•••) was taken 3 h later. At this point, 21 μL of 0.5 M iodoacetamide was added anaerobically, and the spectral course of the reaction was followed. The final reduced, alkylated L40C spectrum (- - -) was recorded 7 h later.

S38C peroxidases. The extinction coefficient at the visible wavelength maximum of 452 nm is 12 mM^{-1} cm^{-1} (Figure 4), and the fluorescence quantum yield of the bound FAD is 22% that of free FAD. In addition, the very low-extinction, long-wavelength absorbance band seen in oxidized wild-type enzyme (Poole & Claiborne, 1989a) is absent. Both the absence of this spectral feature and the enhanced flavin fluorescence of the L40C mutant are similar to properties documented previously with the C42S and C42A proteins (Parsonage & Claiborne, 1995). Thiol assays of the L40C mutant with DTNB give values of 0.07 and 0.04 TNB/FAD under nondenaturing conditions and in the presence of 4 M guanidine, respectively. In contrast, the protein yields 1.1 TNB/FAD in the standard disulfide assay with NTSB in a monophasic reaction ($t_{1/2}$ = 0.3 min). Taken together, these results indicate that substitution of Leu40 with Cys leads to the formation of a disulfide between the new Cys40 and Cys42. Formation of this disulfide, however, does not adversely affect FAD binding as seen with the Cys39–Cys42 disulfide.

The redox properties of the L40C peroxidase and of the Cys40–Cys42 disulfide were assessed in a series of anaerobic reductive titrations. As shown in Figure 4, titration with dithionite leads directly to the two-electron reduced $FADH_2$ enzyme. Immediately on addition of reductant, there is an increase in absorbance over the wavelength range 510–670 nm which is consistent with a small amount of kinetically-stabilized neutral flavin semiquinone; this spectral feature disappears over ~20 min as the semiquinone undergoes dismutation to fully reduced and oxidized species. Complete reduction in this experiment requires 0.8 equiv of dithionite/FAD and yields the anionic reduced flavin spectrum (λ_{max} = 360, 420 nm); there is no evidence for reduction of the Cys40–Cys42 disulfide. The NADH titration shown in Figure 5 also leads to direct reduction of FAD with 1.0 equiv of NADH/FAD, but in this case there is long-wavelength absorbance centered at 790 nm, characteristic of the $FADH_2$ enzyme–NAD^+ complex (Parsonage & Claiborne, 1995). Again, there is no indication of Cys40–Cys42 disulfide reduction; a further 4-h incubation of the reduced enzyme gave no spectral indication of either $FADH_2$ oxidation or disulfide reduction.

The flavin redox potential of the L40C peroxidase was determined by dithionite titration in the presence of the reference dye anthraquinone-2-sulfonate (E'° = −225 mV), with methyl viologen present at low concentration to ensure rapid equilibration of reducing equivalents (Parsonage & Claiborne, 1995). Reduction of the reference dye was monitored at 336 nm, an isosbestic point for oxidized and reduced forms of the protein. Similarly, enzyme reduction was monitored at 354 nm. Following this procedure, a redox potential of −235 mV was determined for the FAD of the L40C mutant; reduction of the Cys40–Cys42 disulfide was not observed. However, when 5 mM DTT was mixed with the L40C peroxidase under anaerobic conditions, a slow spectral change ($t_{1/2}$ ~30 min) ensued as shown in Figure 6. The enzyme species observed at the end of this reaction, with increased long-wavelength absorbance centered at 540 nm, is spectrally very similar to the EH_2 form of wild-type NADH peroxidase. In order to test whether free sulfhydryls

had been generated, iodoacetamide was added anaerobically (3-fold molar excess over DTT); a further increase in absorbance at 540 nm ensued which was complete within 2.5 h. The crystal structure of wild-type NADH peroxidase indicates that the Leu40 side chain is more accessible to solvent than that of Cys42, and earlier attempts to alkylate the reduced Cys42-SH under nondenaturing conditions were unsuccessful (Poole & Claiborne, 1989b). We interpret the sequence of reactions given in Figure 6 as the following: (1) reduction of the Cys40−Cys42 disulfide by DTT, generating the charge-transfer Cys42-SH and the more accessible Cys40-SH, and (2) specific alkylation of Cys40-SH, which also results in an increase in absorbance at 540 nm. This effect of alkylation could reflect either a shift in the redox equilibrium favoring disulfide reduction or an active-site structural change associated with an enhanced Cys42-SH → FAD charge-transfer interaction.

In standard NADH peroxidase assays, the L40C mutant gave initial rates approximately twice the control rate for NADH breakdown (aerobically at pH 5.4). As previously demonstrated with the C42S and C42A proteins, a modified enzyme-monitored approach to steady-state kinetic analysis (Parsonage & Claiborne, 1995; Gibson et al., 1964) provides several advantages when working with peroxidase mutants that have very poor catalytic activity. When 5.8 μM L40C peroxidase was mixed anaerobically with 0.2 mM NADH in the presence of 1 mM H_2O_2, rapid flavin reduction was accompanied by an immediate increase in absorbance at 760 nm, consistent with formation of the L40C $FADH_2$·NAD^+ complex described previously. From these data a turnover number of 0.11 s^{-1}, which is 0.09% that for wild-type enzyme at pH 5.5, was determined.

Mutant Peroxidase S41C. Although the stereochemical constraints on disulfide formation between adjacent cysteines render such −S−S− linkages less common in proteins (Thornton, 1981), several specific examples have been identified. These include the auxiliary disulfide involving Cys628 and Cys629 in mercuric reductase from *Bacillus* sp. RC607 (Schiering et al., 1991) (Cys558 and Cys559 in the enzyme from *Pseudomonas aeruginosa* PAO9501 (Miller et al., 1989)) which, in the reduced form, is thought to contribute one thiol ligand in the binding of Hg(II). While the C^α−C^α and C^β−C^β distances for Ser41 and Cys42 in the wild-type NADH peroxidase are similar to those for Leu40 and Cys42 (Table 2), the Ser41-OG−Cys42-SG distance is 6.6 Å. As purified, the S41C peroxidase appears in the partially-reduced (EH_2) form; titration with H_2O_2 gives the oxidized enzyme, as seen with the S38C mutant. FAD is tightly bound, and the extinction coefficient at 450 nm is 10.8 mM^{-1} cm^{-1}. NADH titration (Figure 7) gives spectral intermediates corresponding to the EH_2 and EH_2·NADH species, and the S41C enzyme has a specific activity (79 units/mg) 65% that of wild-type peroxidase. DTNB titration of the mutant under nondenaturing conditions gives 0.61 TNB/FAD, and thiol/disulfide assay with NTSB yields 0.93 TNB/FAD. Both results are very similar to those obtained with the S38C mutant and fully support the presence of a single free thiol, contributed by Cys41-SH, in the S41C peroxidase.

Crystallographic Analyses of L40C and S41C. The Ramachandran plots (Ramachandran & Sasisekharan, 1968) of the L40C and S41C mutant peroxidases are very similar to that of the wild-type enzyme (Stehle et al., 1991). The

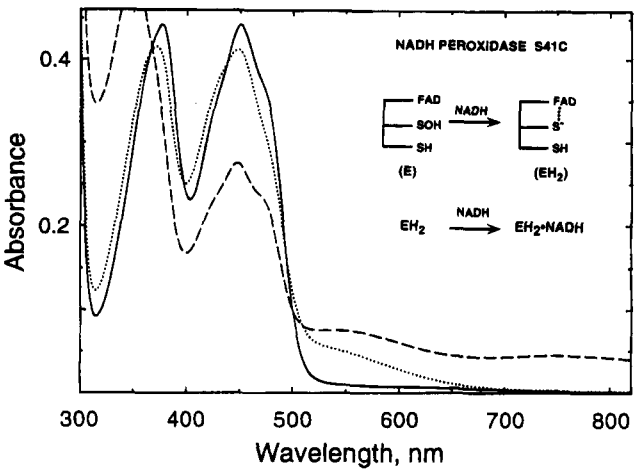

FIGURE 7: Anaerobic NADH titration of the S41C peroxidase. The cuvette contained 29 nmol of enzyme (FAD) in 0.7 mL of the standard phosphate/EDTA buffer, and an oxygen-scrubbing system consisting of protocatechuate dioxygenase and protocatechuic acid (Bull & Ballou, 1981) was added after anaerobiosis. Spectra shown correspond to the addition of 0 (—), 0.65 (• • •), and 1.59 (- - -) equiv of NADH/FAD.

main-chain dihedral angles of residues Lys123 and Phe332, which were found to lie outside favorable regions of the (ϕ,ψ) plot for the wild-type structure, occupy similar deviating positions in the two mutant structures. The final models for the L40C and S41C mutants meet the geometric criteria applied with the program PROCHECK (Laskowski et al., 1993), and the rms deviations in bond lengths, bond angles, impropers, and dihedrals are given in Table 1. Superpositions of the wild-type peroxidase structure with those of L40C and S41C, including all C^α atoms, reveal very similar overall tertiary structures, as expected, with rms C^α deviations of 0.155 and 0.105 Å, respectively. Neither mutation gives rise to any domain movements or rearrangements relative to the wild-type structure.

The active-site structures of the L40C and S41C peroxidases confirm the formation of the Cys40−Cys42 disulfide and the presence of the free Cys41-SH, respectively. Figure 8 gives stereo views of the $2|F_o| - |F_c|$ maps corresponding to these active-site changes. Formation of the Cys40−Cys42 disulfide in L40C leads to significant deviations for these two residues relative to the corresponding Leu40 and Cys42 atoms in the wild-type structure. The maximum deviation, observed for Cys42-SG, is 3.5 Å. The presence of the free Cys41-SH in the active site of the S41C mutant is consistent with the chemical properties of the native protein in solution; the crystal structure of S41C, as with wild-type peroxidase (Stehle et al., 1991), also reveals oxidation of the native Cys42-SOH to the triply oxidized Cys42-SO_3H. It should be emphasized, however, that the Cys41-SG−Cys42-SG interatomic distance is still 6.6 Å. The irreversible oxidation of Cys42 to the sulfonic acid is a unique consequence of the X-ray analysis and does not reflect the oxidation state of Cys42 for the native protein in solution.

In order to visualize the differences in active-site structures of the wild-type and L40C peroxidases, the respective FAD coenzymes were superimposed using the program O (Jones et al., 1991). From the superposition shown in Figure 9, the relative positions of Cys42-SG in the two structures are clearly indicated. While Cys42-SG of the wild-type Cys42-SO_3H is 3.5 Å from the C(4a)-position of the isoalloxazine,

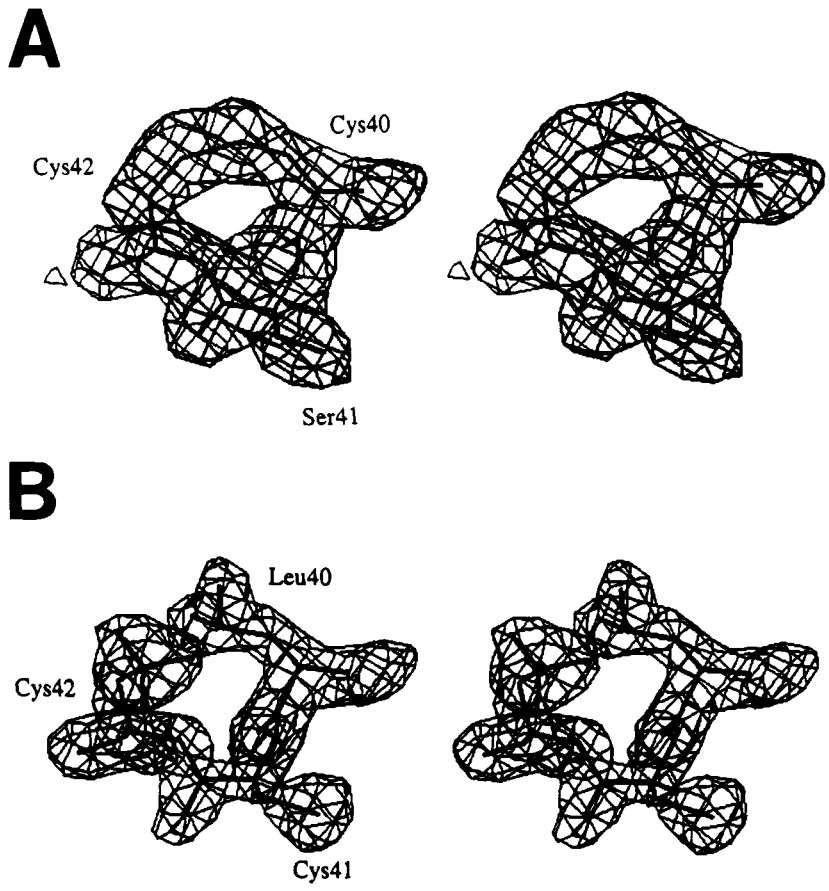

FIGURE 8: Active-site cysteinyl residues as observed in the NADH peroxidase L40C and S41C mutants. Depicted in stereo are the respective $2|F_o| - |F_c|$ maps, generated using the program O (Jones et al., 1991), for (A), the Cys40−Cys42 disulfide of L40C and (B), Cys41-SH and the triply oxidized Cys42-SO_3H of S41C.

Cys42-SG of the L40C disulfide mutant occupies a new position 5.9 Å from the C(4a)-position. In order to further contrast the active-site disulfide of the mutant peroxidase with the redox-active disulfide of glutathione reductase, a similar superposition was performed (Figure 9). While both disulfides present unusual conformational features not commonly found among protein disulfides, only the GR disulfide delivers the charge-transfer Cys63-SG to within 3.5 Å of the corresponding C(4a)-position of the flavin (Karplus & Schulz, 1989). A detailed analysis of the unusual 11-membered ring generated on formation of the Cys40−Cys42 disulfide in the L40C mutant will be published elsewhere.

Finally, the active-site structures of the L40C and S41C mutants are compared in Figure 10. Unlike the substantial deviations in active-site residues observed with the disulfide mutant, relative to wild-type, the maximum deviation in S41C is 0.69 Å, corresponding to the position of Cys41-SG in the mutant protein. While Cys42 is oxidized to the sulfonic acid in the crystal structure of S41C, Cys41 is present as the native Cys41-SH, suggesting that the respective microenvironments of the two cysteines determine their susceptibilities to oxidation during X-ray analysis.

DISCUSSION

The goals of the present study were 2-fold. Our first aim was to introduce a cystine disulfide into the active site of the enterococcal NADH peroxidase, using site-directed mutagenesis. The second component of this plan included a detailed chemical, functional, and structural analysis of those disulfide-containing peroxidase(s) which resulted, allowing a comparison with glutathione reductase. Initially, we made use of multiple sequence alignments of NADH peroxidase and the homologous NADH oxidase (Ross & Claiborne, 1992) with representative members of the GR class of flavoprotein disulfide reductases (Williams, 1992). Ser38 occupies the position in the peroxidase sequence analogous to the GR interchange thiol (Cys42 in the *E. coli* enzyme), and Cys42 of the peroxidase aligns with the charge-transfer cysteine (Cys47) of GR. By combining the information available from the refined structures of the wild-type peroxidase (Stehle et al., 1991) and GR (Mittl & Schulz, 1994; Karplus & Schulz, 1987) with the criteria established by Sowdhamini et al. (1989) for the introduction of disulfide bridges into proteins, we also have access to a rational framework for interpreting the results of our mutagenesis studies. It is important to emphasize that the wild-type peroxidase contains only one half-cystine (Cys42) per polypeptide; the individual replacements of Ser38, Phe39, Leu40, or Ser41 with Cys can lead to only one possible disulfide bridge in each case.

The primary criterion employed for the introduction of disulfide bridges into proteins of known structure requires $C^\alpha-C^\alpha$ and $C^\beta-C^\beta$ distances of ≤ 6.5 and ≤ 4.5 Å, respectively. For the Ser38−Cys42 pair in the peroxidase, both distances exceed 11 Å; this situation contrasts sharply with the $C^\alpha-C^\alpha$ and $C^\beta-C^\beta$ distances of 4.6 and 4.1 Å, respectively, for the Cys42−Cys47 pair in *E. coli* GR, made possible by the unusual distorted helix which includes the redox-active disulfide. It is not surprising that the peroxidase Ser38Cys mutant does not form the corresponding disulfide.

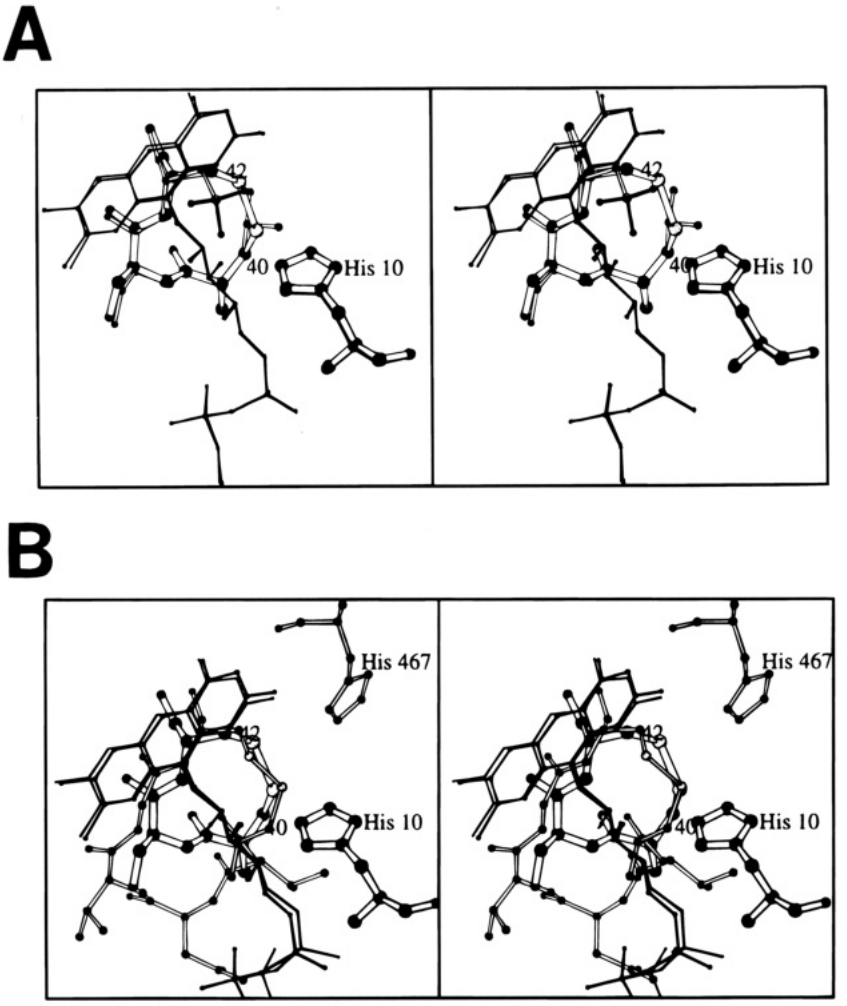

FIGURE 9: The active sites of the L40C peroxidase, wild-type NADH peroxidase, and glutathione reductase. Shown in stereo are MOLSCRIPT (Kraulis, 1991) presentations resulting from the superposition of (A) L40C and wild-type NADH peroxidases and (B) L40C NADH peroxidase and human erythrocyte glutathione reductase. In both cases L40C is represented by thicker bonds, and both of the cysteine positions in the mutant (40 and 42) and His10 are indicated. In (B), His467 corresponds to GR. All atoms of the FAD coenzymes were included in the superpositions, which were carried out using the program O.

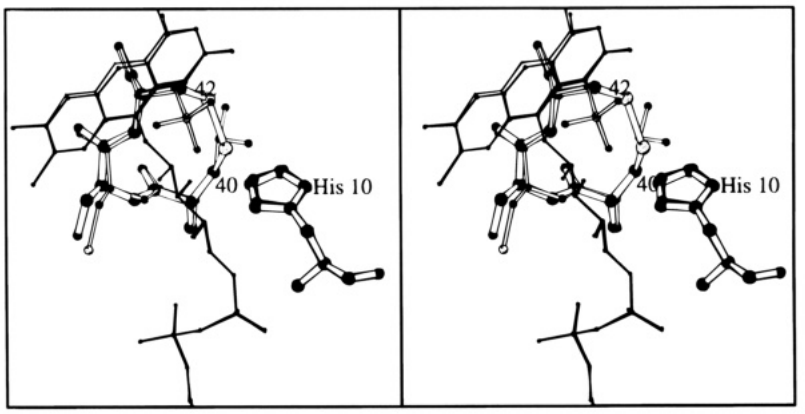

FIGURE 10: Stereoview, generated with MOLSCRIPT, of the superposition of the L40C and S41C peroxidase active sites. L40C is represented by thicker bonds, and both of the cysteine positions in this mutant (40 and 42) and His10 are indicated. All atoms of the FAD coenzymes were included in the superposition, which was carried out using the program O.

By the same token, these distance criteria strongly suggest that replacement of Phe39 with Cys should not lead to formation of the respective Cys39−Cys42 disulfide either. We do, however, observe stoichiometric disulfide formation in the deflavo form of the Phe39Cys mutant, and we have shown that reduction of the disulfide allows tight FAD binding. It should be emphasized, in interpreting these results, that active-site C^{α} and C^{β} coordinates for the wild-type peroxidase, with tightly-bound FAD, cannot be extrapolated to the apo-Phe39Cys protein. At a minimum, we expect the relative Cys39−Cys42 $C^{\beta}-C^{\beta}$ distance to have decreased by at least 5 Å in order for disulfide formation to occur in this mutant. The localized structural perturbation accompanying this movement is most likely also responsible for precluding FAD binding; reduction of the disulfide removes this adverse effect on coenzyme binding and restores

an EH_2-like charge-transfer interaction between Cys42-SH and the FAD.

Sowdhamini et al. (1989), in their inspection of four protein disulfides introduced by site-directed mutagenesis, found that only the $C^\beta-C^\beta$ distance for the Cys3−Cys97 disulfide in T4 lysozyme (4.6 Å) exceeded that distance requirement (≤4.5 Å). The corresponding distance for Leu40 and Cys42 of the peroxidase (5.1 Å) exceeds this limit even further. Our analysis of the active-site structure of the L40C peroxidase clearly shows that significant deviations in the Cys40 and Cys42 residues, relative to Leu40 and Cys42 in the wild-type structure, are necessary in order to accommodate the new Cys40−Cys42 disulfide. The maximum deviation is observed for Cys42-SG (3.5 Å) and results in a movement of the sulfur to a new position 5.9 Å from FAD-C(4a). This contrasts sharply with the favorable 3.5 Å separations observed both for Cys42-SG−FAD-C(4a) in the wild-type peroxidase and for the charge-transfer cysteine and flavin in oxidized GR (Karplus & Schulz, 1989). The proximity of these equivalent cysteine residues in the sulfenic acid (NADH peroxidase) and disulfide (GR) redox centers to the isoalloxazine moiety is critical to their catalytic functions, since the flavin mediates reduction by NAD(P)H in each case. In the L40C peroxidase the unfavorable Cys42-SG−FAD-C(4a) separation is entirely consistent with the observed lack of $FADH_2$ → disulfide electron transfer and the virtual elimination of catalytic activity. We have previously shown that direct $FADH_2$-mediated reduction of H_2O_2 accounts for the very low turnover rates observed with the C42S and C42A mutant peroxidases (Parsonage & Claiborne, 1995), and a similar process is likely to account for the very poor activity of the L40C mutant, since NADH reduction of the flavin is rapid.

It has also been pointed out (Sowdhamini et al., 1989) that the mutant disulfides introduced into dihydrofolate reductase, T4 lysozyme, and subtilisin are stereochemically "nonoptimal"; the inherent strain in the subtilisin Cys22−Cys87 and Cys24−Cys87 disulfides was confirmed by X-ray crystallography (Katz & Kossiakoff, 1986). Independent analyses (Katz & Kossiakoff, 1986; Wells & Powers, 1986) of these two mutants also demonstrated that the respective dihedral energies could be correlated with the disulfide/dithiol redox potentials. Karplus and Schulz (1987) and Mattevi et al. (1991) have demonstrated that the redox-active disulfides in GR and lipoamide dehydrogenase also exhibit unusual strained conformations that translate into more facile reduction of $E \rightarrow EH_2$. The corresponding redox potentials are −243 mV (Veine et al., 1994) and −280 mV (Matthews & Williams, 1976), respectively, and in both cases the non-flavin center is preferentially reduced in static titrations. Similarly, the potential for the Cys42-SOH redox center in wild-type NADH peroxidase is at least 86 mV more positive than that for the flavin (Poole & Claiborne, 1989b). Titrations of the L40C mutant, however, consistently show direct flavin reduction by NADH or dithionite, with no evidence for reduction of the Cys40−Cys42 disulfide even in the presence of the redox communicator methyl viologen. The structure of the L40C peroxidase shows that the mutant disulfide does exhibit an unusual conformation which might be expected to facilitate reduction, and independent experiments show that DTT, when present in large excess, will reduce the disulfide slowly under anaerobic conditions. Further considerations of the unusual stereochemical features of the L40C mutant disulfide and its redox properties will be given in a separate report. The flavin potential of −235 mV determined for L40C compares favorably with those of the C42S and C42A mutants (−219 and −197 mV (Parsonage & Claiborne, 1995)); in all three cases the potentials are at least 80 mV more positive than that of the wild-type EH_2 flavin, consistent with the absence of Cys42-SH → FAD charge-transfer interaction in each of the mutants.

The Ser41−Cys42 $C^\beta-C^\beta$ distance in the wild-type peroxidase also exceeds one of the criteria for disulfide introduction in the S41C mutant, and the chemical and functional analyses of the expressed protein confirm the absence of a Cys41−Cys42 disulfide. The distance between the two cysteine sulfurs, determined from the S41C crystal structure, is 6.6 Å and clearly precludes disulfide bridge formation. The crystal structure also demonstrates that, although Cys41-SH is accessible to solvent, only the Cys42 side chain is oxidized to the non-native sulfonic acid derivative. This suggests that specific factors relating to the Cys42 microenvironment actually promote the further irreversible oxidation of this cysteine during X-ray analysis. While such oxidation was not observed for either the interchange or charge-transfer thiols of GR in the X-ray analysis of the EH_2•NADH complex (Karplus & Schulz, 1989), similar active-site cysteine oxidations have been observed during crystallographic studies of the thiol proteases papain (Kamphuis et al., 1984) and actinidin (Baker, 1980) and the related enzyme dienelactone hydrolase (Pathak & Ollis, 1990). The strongly acidic $-SO_2H$ (sulfinic acid) and $-SO_3H$ (sulfonic acid) derivatives which result in these cases appear to be formed readily in the thiol proteases owing to the adjacent oxyanion binding sites in which one of the new oxygen atoms binds. The structures of the NADH peroxidase C42S and C42A mutants (Mande et al., 1995) reveal the presence of a tightly-bound active-site water which interacts with five hydrogen-bond partners. In the wild-type Cys42-SO_3H structure, one of the sulfonic acid oxygens displaces this water and participates in a similar hydrogen-bonding network (Stehle et al., 1991, 1993). These observations are consistent with the presence of a site near Cys42 in the peroxidase which is similar to the thiol protease oxyanion binding site and may contribute to the ready formation of the Cys42-SO_3H derivative seen in the wild-type and S41C crystal structures.

NADH peroxidase and GR require the same intimate working relationship between a proximal cysteine and the flavin for their catalytic redox functions. In this work we have demonstrated that the two enzymes are optimally designed to accommodate and deploy Cys-SOH and Cys−Cys redox centers in their respective reductions of the small polar H_2O_2 and the dimeric tripeptide disulfide represented by GSSG.

ACKNOWLEDGMENT

We would like to thank Randy Bledsoe for his contributions to the expression and analysis of the NADH peroxidase S41C mutant.

REFERENCES

Bailey, J. L. (1962) in *Techniques in Protein Chemistry*, pp 294−295, Elsevier Scientific Publishing Co., New York.
Baker, E. N. (1990) *J. Mol. Biol. 141*, 441−484.

Brünger, A. T., Kuriyan, J., & Karplus, M. (1987) *Science 235*, 458−460.
Bull, C., & Ballou, D. P. (1981) *J. Biol. Chem. 256*, 12673−12680.
Claiborne, A., Ross, R. P., & Parsonage, D. (1992) *Trends Biochem. Sci. 17*, 183−186.
Claiborne, A., Miller, H., Parsonage, D., & Ross, R. P. (1993) *FASEB J. 7*, 1483−1490.
Claiborne, A., Ross, R. P., Ward, D., Parsonage, D., & Crane, E. J., III (1994) in *Flavins and Flavoproteins 1993* (Yagi, K., Ed.) pp 587−596, de Gruyter, New York.
Devereux, J., Haeberli, P., & Smithies, O. (1984) *Nucleic Acids Res. 12*, 387−395.
Gibson, Q. H., Swoboda, B. E. P., & Massey, V. (1964) *J. Biol. Chem. 239*, 3927−3934.
Greer, S., & Perham, R. N. (1986) *Biochemistry 25*, 2736−2742.
Hall, S. R., & Stewart, J. M., Eds. (1987) *XTAL2.2 User's Manual*, Universities of Western Australia and Maryland.
Higgins, D. G., & Sharp, P. M. (1988) *Gene 73*, 237−244.
Howard, A. J., Gilliland, G. L., Finzel, B. C., Poulos, T. L., Ohlendorf, D. M., & Salemme, F. R. (1987) *J. Appl. Crystallogr. 20*, 383−387.
Jones, T. A., Zou, J. Y., & Cowan, S. W. (1991) *Acta Crystallogr. A47*, 110−119.
Kamphuis, I. G., Kalk, K. H., Swarte, M. B. A., & Drenth, J. (1984) *J. Mol. Biol. 179*, 233−256.
Karplus, P. A., & Schulz, G. E. (1987) *J. Mol. Biol. 195*, 701−729.
Karplus, P. A., & Schulz, G. E. (1989) *J. Mol. Biol. 210*, 163−180.
Katz, B. A., & Kossiakoff, A. (1986) *J. Biol. Chem. 261*, 15480−15485.
Kraulis, P. J. (1991) *J. Appl. Crystallogr. 24*, 946−950.
Laddaga, R. A., Chu, L., Misra, T. K., & Silver, S. (1987) *Proc. Natl. Acad. Sci. U.S.A. 84*, 5106−5110.
Laskowski, R. A., MacArthur, N. W., Moss, D. S., & Thornton, J. M. (1993) *J. Appl. Crystallogr. 26*, 283−290.
Mande, S. S., Parsonage, D., Claiborne, A., & Hol, W. G. J. (1995) *Biochemistry* (submitted for publication).
Mattevi, A., Schierbeek, A. J., & Hol, W. G. J. (1991) *J. Mol. Biol. 220*, 975−994.
Matthews, R. G., & Williams, C. H., Jr. (1976) *J. Biol. Chem. 251*, 3956−3964.
Miller, H., & Claiborne, A. (1991) *J. Biol. Chem. 266*, 19342−19350.
Miller, S. M., Moore, M. J., Massey, V., Williams, C. H., Jr., Distefano, M. D., Ballou, D. P., & Walsh, C. T. (1989) *Biochemistry 28*, 1194−1205.
Mittl, P. R. E., & Schulz, G. E. (1994) *Protein Sci. 3*, 799−809.
Parsonage, D., & Claiborne, A. (1995) *Biochemistry 34*, 435−441.
Parsonage, D., Miller, H., Ross, R. P., & Claiborne, A. (1993) *J. Biol. Chem. 268*, 3161−3167.
Pathak, D., & Ollis, D. (1990) *J. Mol. Biol. 214*, 497−525.
Poole, L. B., & Claiborne, A. (1986) *J. Biol. Chem. 261*, 14525−14533.
Poole, L. B., & Claiborne, A. (1988) *Biochem. Biophys. Res. Commun. 153*, 261−266.
Poole, L. B., & Claiborne, A. (1989a) *J. Biol. Chem. 264*, 12330−12338.
Poole, L. B., & Claiborne, A. (1989b) *J. Biol. Chem. 264*, 12322−12329.
Ramachandran, G. N., & Sasisekharan, V. (1968) *Adv. Protein Chem. 23*, 283−437.
Read, R. J. (1986) *Acta Crystallogr. A42*, 140−149.
Riddles, P. W., Blakeley, R. L., & Zerner, B. (1979) *Anal. Biochem. 94*, 75−81.
Ross, R. P., & Claiborne, A. (1991) *J. Mol. Biol. 221*, 857−871.
Ross, R. P., & Claiborne, A. (1992) *J. Mol. Biol. 227*, 658−671.
Schiering, N., Kabsch, W., Moore, M. J., Distefano, M. D., Walsh, C. T., & Pai, E. F. (1991) *Nature 352*, 168−172.
Shames, S. L., Kimmel, B. E., Peoples, O. P., Agabian, N., & Walsh, C. T. (1988) *Biochemistry 27*, 5014−5019.
Sowdhamini, R., Srinivasan, N., Shoichet, B., Santi, D. V., Ramakrishnan, C., & Balaram, P. (1989) *Protein Eng. 3*, 95−103.
Stehle, T., Ahmed, S. A., Claiborne, A., & Schulz, G. E. (1991) *J. Mol. Biol. 221*, 1325−1344.
Stehle, T., Claiborne, A., & Schulz, G. E. (1993) *Eur. J. Biochem. 211*, 221−226.
Stephens, P. E., Lewis, H. M., Darlison, M. G., & Guest, J. R. (1983) *Eur. J. Biochem. 135*, 519−527.
Thannhauser, T. W., Konishi, Y., & Scheraga, H. A. (1984) *Anal. Biochem. 138*, 181−188.
Thieme, R., Pai, E. F., Schirmer, R. H., & Schulz, G. E. (1981) *J. Mol. Biol. 152*, 763−782.
Thornton, J. M. (1981) *J. Mol. Biol. 151*, 261−287.
Veine, D. M., Arscott, L. D., & Williams, C. H., Jr. (1994) in *Flavins and Flavoproteins 1993* (Yagi, K., Ed.) pp 497−500, de Gruyter, New York.
Wells, J. A., & Powers, D. B. (1986) *J. Biol. Chem. 261*, 6564−6570.
Wierenga, R. K., Terpstra, P., & Hol, W. G. J. (1986) *J. Mol. Biol. 187*, 101−107.
Williams, C. H., Jr. (1992) in *Chemistry and Biochemistry of Flavoenzymes* (Müller, F., Ed.) Vol. III, pp 121−211, CRC Press, Boca Raton, FL.

BI942872H